Journal of Reproduction and Development, Vol. 66, No 6, 2020

—Original Article—

Unique morphological characteristics in the ovary of cotton rat (*Sigmodon hispidus*)

Md. Rashedul ISLAM[1, 2], Osamu ICHII[1, 3], Teppei NAKAMURA[1, 4], Takao IRIE[5], Md. Abdul MASUM[1, 6], Marina HOSOTANI[7], Yuki OTANI[1], Yaser Hosny Ali ELEWA[1, 8] and Yasuhiro KON[1]

[1]*Laboratory of Anatomy, Department of Basic Veterinary Sciences, Faculty of Veterinary Medicine, Hokkaido University, Hokkaido 060-0818, Japan*
[2]*Department of Surgery and Theriogenology, Faculty of Animal Science and Veterinary Medicine, Sher-e-Bangla Agricultural University, Dhaka 1207, Bangladesh*
[3]*Laboratory of Agrobiomedical Science, Faculty of Agriculture, Hokkaido University, Hokkaido 060-0818, Japan*
[4]*Section of Biological Safety Research, Chitose Laboratory, Japan Food Research Laboratories, Hokkaido 060-0818, Japan*
[5]*Medical Zoology Group, Dept. of Infectious Diseases, Hokkaido Institute of Public Health, Hokkaido 060-0818, Japan*
[6]*Department of Anatomy, Histology and Physiology, Faculty of Animal Science and Veterinary Medicine, Sher-e-Bangla Agricultural University, Dhaka 1207, Bangladesh*
[7]*Laboratory of Anatomy, School of Veterinary Medicine, Rakuno Gakuen University, Hokkaido 060-0818, Japan*
[8]*Department of Histology, Faculty of Veterinary Medicine, Zagazig University, Zagazig 44519, Egypt*

Abstract. Cotton rats (*Sigmodon hispidus*, CRs) are commonly used as animal models in biomedical research. However, the reproductive characteristics and ovarian development in the CRs has not been widely investigated. We have previously shown that female CRs, in particular, show several unique phenotypes associated with the urogenital system, such as chronic kidney disease and pyometra. Our investigation revealed unique morphologies in CR ovaries, particularly in oocytes. Cotton rat ovaries at 6–8 weeks of age were obtained from the Hokkaido Institute of Public Health, and their sections analyzed by light microscopy and transmission electron microscopy. Although the general histology and folliculogenesis of CR ovaries were similar to those of other experimental rodents, multi-oocyte follicles (MOFs) and double nucleated oocytes (DNOs) were also observed. Although MOFs were found at all stages of follicular development, a greater frequency of MOFs was observed in the primary and secondary stages. However, DNOs tended to be frequently observed in primordial follicles. Almost all MOF oocytes and a few DNOs possessed a clear zona pellucida, expressed DEAD (Asp-Glu-Ala-Asp) box polypeptide 4 and Forkhead box protein 2, a representative marker of oocytes and follicular epithelial cells. Thus, our investigations revealed the unique phenotypes of the CR ovary. As MOFs and DNOs are occasionally observed in human patients with infertility, the CR would be a useful animal model to study for gaining a better understanding of folliculogenesis and oocytogenesis, as well as their abnormalities in humans and other animals.

Key words: Cotton rat, Double nucleated oocytes, Folliculogenesis, Multi-oocyte follicles, Oocytogenesis

(**J. Reprod. Dev. 66:** 529–538, 2020)

Infertility is a common reproductive health problem creating socioeconomic complications in humans and animals alike. Fertility depends on normal morpho-functional activities of the ovaries, which are the primary organs responsible for reproduction, and act as a reservoir of follicles. The ovarian follicle is a morpho-functional unit containing a germ cell surrounded by somatic cells arranged in a single or multiple layer, according to the follicle developmental stage [1]. In the mouse, follicular development from primordial to antral begins at the early postnatal development stage and continues until the late term of the life span [2]. Significant efforts have been made in recent years to elucidate the factors and mechanisms regulating folliculogenesis, since the size of the primordial follicle (PrF) population is determined, at least partly, by the reproductive life span of female mammals.

Folliculogenesis is a key component of reproductive physiology, although some aspects of this process remain unclear, such as the appearance of the multi-oocyte follicles (MOFs), which are structures with two or more oocytes contained within a single follicle [3]. Although most follicles contain only one oocyte as single oocyte follicles (SOFs), the presence of MOFs containing two or more oocytes has been described in several animal species, showing large species-related differences such as in cattle [4, 5], dogs [1, 6], pigs [7, 8], sheep [9, 10] and goats [11]. It has been hypothesized that these follicles are formed in the early stages of folliculogenesis and develop from a natural polymorphism that results in oocyte rearrangements [5, 8]. Another hypothesis posits that these follicles are derived

Received: May 11, 2020
Accepted: August 17, 2020
Advanced Epub: September 3, 2020

Correspondence: Y Kon (e-mail: y-kon@vetmed.hokudai.ac.jp)

from a failure to separate the germ cells during the early phases of folliculogenesis [12] or also from the inclusion of various germ cells within a follicle [13]. Apart from their contentious origins, not much is well understood regarding the development of MOFs. The significance of the characteristics of MOFs remains unclear as well.

The cotton rat (CR) is an experimental rodent with seven subspecies, with only *Sigmodon hispidus* originating from the southern United States. This subspecies is well characterized and is commonly used in biomedical research [14]. Reproductive characteristics of the CR have been fairly extensively studied. Moreover, CR is prolific in nature and produces nine litters per year, averaging at five to six puppies per litter [14]. Our previous studies revealed unique phenotypes in CRs such as metabolic disorder and pharyngeal pouch remnants and those associated with the urogenital system such as chronic kidney disease and pyometra [15].

In the present study, we investigated the morphological characteristics of CRs using histological techniques. Briefly, the general histology and folliculogenesis in CR ovaries were similar to those in other experimental rodents. On the other hand, the CR ovary contained several MOFs as well as the double nucleated oocytes (DNOs). MOFs had two or more oocytes encased in a single follicle without a separating basement membrane among the follicles, and DNOs had two nuclei encased in a single follicle containing oocytes. As MOFs and DNOs are occasionally observed in human patients with infertility [16], CRs could be used as an appropriate model to study folliculogenesis and oocytogenesis in humans, and our findings could be extended to human biomedical research as well.

Materials and Methods

Animals and tissue processing

Animal experimentation was performed according to the guidelines of the Hokkaido Institute of Public Health (approval no.: K27-03) and the Faculty of Veterinary Medicine, Hokkaido University (approval no.: 20-0012). The CRs were 6–8 weeks old, previously classified as the young period [15]. They were maintained as the HIS/Hiph strain through continuous inbreeding under conventional conditions at the Hokkaido Institute of Public Health (Sapporo, Japan). Moreover, 6-week-old inbred C57BL/6N and outbred Jcl:ICR (ICR) mice were obtained from Japan SLC (Hamamatsu, Japan). All mice were maintained in specific pathogen-free conditions, and food and water were provided *ad libitum*. They were euthanized by cutting the abdominal aorta under deep anesthesia with isoflurane. The harvested ovaries were fixed with 10% neutral buffer formalin (NBF), 4% paraformaldehyde (PFA), or 2.5% glutaraldehyde (GTA) in 0.1 M phosphate buffer (PB) for histological analysis, immunohistochemical stainings, and ultrastructural analysis, respectively.

Light microscopy and histoplanimetry

Paraffin-embedded blocks of 5 ovarian specimens were cut at a thickness of 5 µm to obtain whole ovarian semi-serial sections and stained with Hematoxylin-Eosin (HE) or periodic acid Schiff-hematoxylin (PAS-H) to examine the morphological characteristics of the CR ovarian follicles. The stained slide glasses were scanned by the NanoZoomer 2.0 RS virtual slide scanner (Hamamatsu Photonics, Shizuoka, Japan), and the data were used for histoplanimetry. Then, BZ-X710 microscopy (Keyence, Osaka, Japan) was used to obtain the histological images.

For histoplanimetry using HE stained sections, ovarian follicles were classified, based on their stages, as PrF, primary (PF), secondary (SF), and tertiary follicles (TF), according to previously reported studies in rabbits [17]. Their numbers were counted at 7-section intervals (whole ovaries were sectioned, resulting in at least 50 sections per ovary), and the number of various developmental follicles was multiplied by 7 to get an assessment of the total number of follicles per ovary [18, 19]. Only follicles containing visible oocytes were counted to avoid double counting. In brief, PrFs had an oocyte surrounded by a single layer of flattened follicular epithelial cells. However, PFs were identified as an oocyte enclosed by a layer of granulosa cells (GCs). Secondary follicles contained two or three layers of GCs surrounding the oocyte, but there was no visible antral cavity among follicular epithelial cells. Tertiary follicles, having small follicular spaces between follicular epithelial cells, began to form and these follicles were composed of four or more granular layers.

The developmental stage of ovarian follicles containing more than 2 oocytes (defined as MOFs) or 2 nuclei (defined as DNOs) were classified according to the above criteria [17], and their numbers were counted. The percentage of MOFs or ovarian follicles containing DNOs among all follicles was also calculated.

For the determination of oocyte polarity, 10 PFs and SFs containing single and multiple oocytes were randomly selected from each ovarian specimen. Selected oocytes were split by a line passing by the center of the nucleus with the NDP.view2 software, and such a line was divided into two sections, indicating the long distance (LD) and short distance (SD) between the nuclear membrane and the plasma membrane of oocytes. Measurements were taken for both LD and SD.

Immunohistochemistry

Immunohistochemical staining for the oocyte marker DEAD (Asp-Glu-Ala-Asp) box polypeptide 4 (Ddx4), and the follicular epithelial cell marker Fork head box protein 2 (Foxl2), were performed to estimate whether the oocytes of CRs, in particular those in MOFs or DNOs, show biological characteristics similar to those of other rodents. Ddx4 and Foxl2 were expressed in germ cells and follicular epithelial cells from the time of their first appearance to adulthood in mice [20]. Furthermore, Ki-67 was used to observe the proliferative activity of developing follicles. Briefly, deparaffinized sections were treated with 10 mM citrate buffer for 20 min at 105°C for antigen retrieval, and then incubated in 0.3% H_2O_2/methanol solution for 10 min to quench the endogenous peroxidase activity. The sections were then blocked with 10% normal goat serum (SABPO kit; Nichirei Bioscience, Tokyo, Japan) for Ddx4 and Ki-67 stainings and 5% normal donkey serum for Foxl2 stainings. They were incubated overnight with rabbit anti-Ddx4 antibody (1: 500; Abcam, Cambridge, UK), anti-Ki-67 antibody (1: 800; Abcam), and biotinylated donkey anti-goat IgG antibody (1:400; Santa Cruz, Dallas, TX, USA) at 4°C. The sections were then treated with biotinylated goat anti-rabbit IgG (SABPO kit, Nichirei Bioscience) for 30 min at room temperature. This was followed by streptavidin-horseradish peroxidase (SABPO kit; Nichirei, Tokyo, Japan) incubation for 30 min followed by incubation with 3,3-diaminobenzidine tetrahydrochloride-H_2O_2

solution. Finally, the sections were counterstained with hematoxylin and dehydrated with ascending grades of alcohol. The stained sections were examined under a BZ-X710 microscope (Keyence).

Electron microscopy

The CR ovaries were immediately fixed with 2.5% GTA in 0.1 M PB for 4 h, at 4°C, followed by post-fixation with 1% osmium tetroxide (OsO_4) in 0.1 M PB for 2 h. The specimens were then dehydrated with ascending grades of alcohol and embedded in epoxy resin (Quetol 812 Mixture; Nisshin EM, Tokyo, Japan). The epoxy blocks were cut at a thickness of 60 nm. Approximately, 80-100 ultrathin sections (at least 10 sections from each ovary) were mounted on grids. The sections were stained with uranyl acetate and lead citrate for 15 min and 10 min, respectively. The stained sections were observed under a transmission electron microscope (TEM) (JEM-1210; JEOL, Tokyo, Japan).

Statistical analysis

The results were expressed as mean ± standard error (SE) and were analyzed using nonparametric methods. Two groups were compared using the Mann-Whitney *U*-test. The Kruskal-Wallis test was used to compare the developmental stages of 3 or more follicle groups with MOFs or DNOs, and multiple comparisons were performed using Scheffé's method.

Results

General histology of the CR ovary

Figure 1 shows the histological characteristics of the CR ovary. The ovarian cortex and medulla, developmental ovarian follicles, and the corpus luteum were observed in the cortex, similar to other rodent species (Fig. 1a). Furthermore, the follicles which progressed to later developmental stages, such as SF, localized to the superficial or deep region of the cortex, as previously reported in rodents [21] or rabbits [17]. Moreover, the interstitial gland, a characteristic of the rodent ovary [22], was observed throughout the cortical stroma (Fig. 1b) and clusters of epithelioid cells resembled luteal cells in the magnified area of panel b.

We then classified the developmental stages of the ovarian follicles according to the morphology of the follicular epithelium or granular layers, as mentioned in the materials and methods section [17]. According to that criteria, the developmental follicles were classified as PrF, PF, SF, and TF (Fig. 1c–f).

For histoplanimetry (Table 1), the follicle number at each developmental stage decreased as follicular development progressed. PrF showed the highest number and percentage of follicles, and a significant difference was detected compared with those of TF ($P < 0.01$). PrF also showed the higher percentage of follicles compared to SF ($P < 0.01$). PF showed a significantly higher number ($P < 0.05$) and percentage ($P < 0.01$) of follicles compared to TF. Further, PF showed a significantly higher percentage of follicles compared to SF ($P < 0.01$).

MOFs in the CR ovary

A MOF is defined as an SOF containing two or more oocytes (Fig. 2). The CR ovary showed MOFs in all the developmental stages of follicles, including PrF, PF, SF, and TF (Fig. 2a–d). MOFs classified as PrF (Fig. 2a) were similar to oocyte nests as found in prenatal or neonatal ovaries [3]. In particular, the zona pellucida was clearly observed in MOFs classified as SF or TF, similar to single oocyte follicles (Fig. 2c and d). The MOFs frequently observed in histology images seemed to be unique histological features of the CR ovary. Indeed, when observing the ovaries of C57BL/6N ($n = 4$) and ICR ($n = 4$) mice, we detected no MOFs in the ovary of C57BL/6N mice (Supplementary Fig. 1a: online only) but found only two MOFs, one in a SF and another in a TF, in ovaries of ICR mice (Supplementary Fig. 1c–d).

In Table 2, the highest number of MOFs was observed in those classified as PF, compared to that observed in other developmental stages of the ovarian follicle in the histoplanimetric analysis. Significant differences were observed in PF and SF compared with PrF and TF MOFs ($P < 0.01$). Furthermore, MOFs classified as SF also showed significantly higher values compared with those of TF ($P < 0.01$), while the percentage of MOFs classified as SF was higher compared with the percentage of those classified as PrF, PF and TF.

Most MOFs had 2 oocytes in a single follicle, but some of them had 3 or more (Fig. 3a–c). The sizes of MOFs were 2 to 3 times larger compared to the follicles containing single oocytes because of the increased number of oocytes and GCs. The shape of the MOFs in CRs also showed morphological variation, especially those in PrF, which were elongated, triangular, or rounded (Fig. 3a). The oocytes of MOFs seemed to be separated by follicular epithelial cells or granulosa cells (Fig. 3c). An observation of semi-serial sections showed that the apparently single follicles (Fig. 3d and e) in one section were connected to MOFs in the next section (Fig. 3f), indicating that some MOFs have fine interconnections via GCs.

Characterization of SOFs and MOFs by immunostaining

We immunohistochemically examined the expression of the pan-oocyte marker Ddx4 and the follicular epithelial marker Foxl2 in the CR ovary. In mice, Ddx4 and Foxl2 are expressed in germ cells and the nuclei of follicular epithelial cells from the time of their first appearance to adulthood [20]. As shown in Figure 3g–i, in addition to the single follicles (Fig. 3g and i), the cytoplasm of oocytes in the MOFs classified as PrF (Fig. 3g), PF (Fig. 3h), SF and TF (Fig. 3i) showed positive expression for Ddx4. Furthermore, the oocyte nucleus in MOFs showed polarity of localization in the cytoplasm (Fig. 3g–i). As shown in Table 4, the measured LD between the nuclear membrane and the plasma membrane of oocytes in PFs and SFs containing single and multiple oocytes was significantly greater than the respective SD ($P < 0.01$). Moreover, Foxl2 expression was observed in the nuclei of follicular epithelial cells in SOFs (Fig. 3j) and MOFs (Fig. 3k–l). The theca cell layer starts to develop from SF onward. However, Ki-67 staining demonstrated the proliferative activity of GCs, but not of oocytes, in the follicles (Supplementary Fig. 2a–c: online only). The majority of the MOFs had been developed before the formation of the theca cell layer. However, the role of theca cells in follicular function has received less attention compared with intensive investigations into the role of granulosa cells [23]. The thickness of the theca cell layer depends on the type of follicles. There were no visible differences in theca cell layer thickness between SOFs and MOFs, with SF and TF having SOFs (Fig. 3m), MOFs in

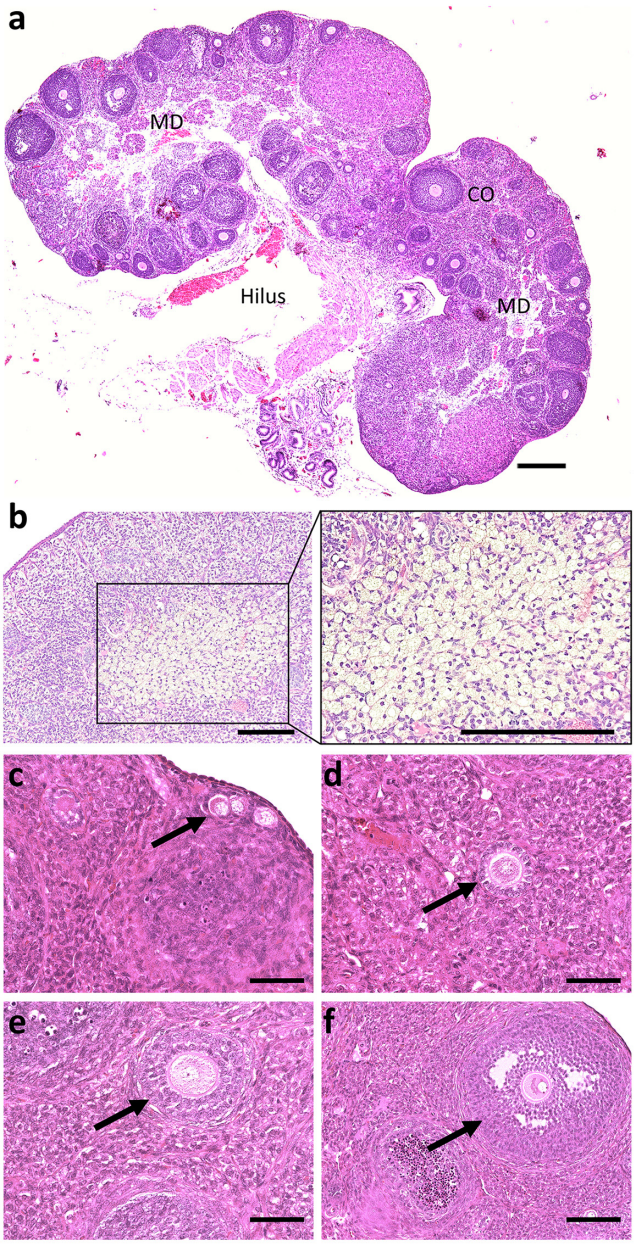

Fig. 1. General histology of the ovary of cotton rats (CRs). (a–g) Histological observation of hematoxylin eosin-stained ovary section from CR at 6–8 weeks of age. The ovarian cortex (CO) and medulla (MD) are clearly observed in the CR ovary, and the vascular system entering the ovarian hilus (panel a). Panel b shows the interstitial glands. Panels c, d, e, and f show primordial (PrF), primary (PF), secondary (SF), and tertiary follicles (TF), respectively. Arrows in panels c-f indicate the PrF, PF, SF, and TF, respectively. Scale bar = 100 µm.

SF (Fig. 3n) and TF (Fig. 3o).

DNOs in the CR ovary

In addition to MOFs, we found another unique characteristic of the CR ovary, DNOs, which are oocytes with two nuclei encased in a single follicle. Figure 4 shows the appearance of DNOs, containing two nuclei, in developing follicles including PrF (Fig. 4a), PF (Fig. 4b), and SF (Fig. 4c). The nuclei are closely attached (Fig. 4a–b) or separated (Fig. 4c) within the same cytoplasm of follicles. Normally, SOF contained single nucleus and size of the nucleus seemed to be largest in initial stages as PrF (Fig. 4d). The majority of them were found in PrF which was beneath the peripheral area and the remaining DNOs lied either superficially or deep in the cortex of CR ovaries. Notably, mature follicles such as TF did not contain any DNOs (Fig. 4d and e). DNOs also showed Ddx4-positivity in the cytoplasm of PrF, PF and SF (Fig. 4d–f), respectively.

The histoplanimetric data for DNOs are shown in Table 3. Briefly, from all the examined sections, the PrF showed the highest number of DNOs, while the number of DNOs was sharply decreasing in

Table 1. The total number and percentage of each developmental follicle in the cotton rat (CR) ovary

Follicle stage	PrF	PF	SF	TF
Total number	332.0 ± 25.4 $^{b'}$	203.6 ± 27.6 ^{b}	104.8 ± 12.1	23.2 ± 3.1
Percentage (%)	48.6 ± 1.2 $^{a', b'}$	30.3 ± 1.0 $^{a, b'}$	15.9 ± 0.9	3.5 ± 0.5

Values are mean ± SE. The letters (a and b) denote statistical significance with secondary (SF) and tertiary follicles (TF), (Kruskal-Wallis test followed by Scheffe's method, $P < 0.05$). The dash beside the letters indicates highly significant differences compared to TF ($P < 0.01$). n = 5 ovaries (at least 50 sections/ovary).

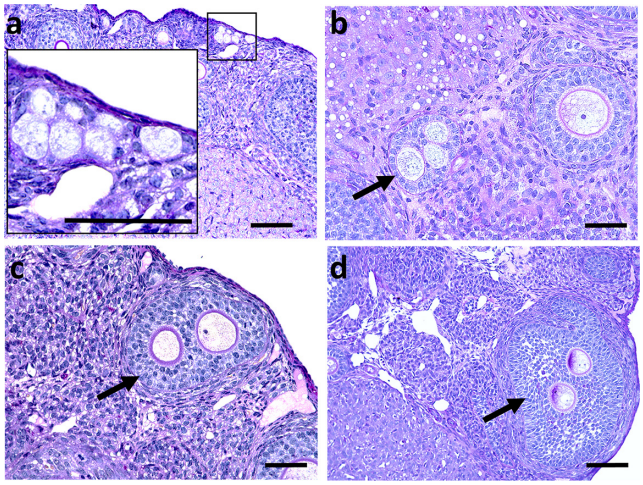

Fig. 2. Appearance of multi-oocyte follicles in the ovary of cotton rats (CRs). (a–d) Histological observation of periodic acid Schiff-hematoxylin (PAS-H)- stained ovary section in the CR at 6–8 weeks of age. Multi-oocyte follicles (MOF) are observed in the CR ovary, and are classified as primordial (PrF), primary (PF), secondary (SF), and tertiary follicles (TF) (panels a–d, respectively). Square area in panel a indicate the same area of the inset. Arrows in panel b–d indicate the PF, SF and TF, respectively. In panel b–d, Periodic acid Schiff-hematoxylin (PAS-H)-positive zonae pellucidae are clearly observed. Scale bar = 100 µm.

Table 2. The total number and percentage of multi-oocyte follicles (MOFs) classified by the stage of follicular development in the cotton rat (CR) ovary

Follicle stage	PrF	PF	SF	TF
Total number	7.2 ± 0.8	18.8 ± 2.1 $^{a', b'}$	11.8 ± 1.6 $^{b'}$	0.6 ± 0.2
Percentage (%)	2.2 ± 0.4	9.8 ± 1.8 $^{a, b}$	11.7 ± 1.9 $^{a, b}$	2.4 ± 1.0

Values are mean ± SE. The letters (a and b) denote statistical significance with primordial (PrF) and tertiary follicles (TF), (Kruskal-Wallis test followed by Scheffe's method, $P < 0.05$). The dash beside the letters indicates highly significant differences compared with PrF and TF ($P < 0.01$). n = 5 ovaries (at least 50 sections/ovary).

Table 3. The total number and percentage of double nucleated oocytes (DNOs) classified by the stage of follicular development in the cotton rat (CR) ovary

Follicle stage	PrF	PF	SF	TF
Total number	1.4 ± 0.3	0.6 ± 0.3	0.2 ± 0.2	ND
Percentage (%)	0.4 ± 0.1	0.2 ± 0.2	0.1 ± 0.2	

Values are mean ± SE. ND: not detected. n = 5 ovaries (at least 50 sections/ovary).

the consecutive follicles. However, no significant differences were detected. Furthermore, while no significant differences were observed, the percentage of DNOs in each follicular stage appeared to be higher in PrF compared to that in other types of follicles. We did not find any DNOs in ovaries of C57BL/6N and ICR mice.

Ultrastructure analysis of CR ovary

Figure 5 shows the ultrastructural analysis of follicles by TEM. Figure 5a shows a representative image of a PrF having a single oocyte. It has a clear round-shaped nucleus, and the mitochondrial clouds of the CR oocyte have a unique structure. Indeed, the mitochondrial clouds are distributed throughout the cytoplasm of the oocyte. On the other hand, the oocytes in MOFs classified as PrF were separated by follicular epithelial cells (Fig. 5b). Moreover, mitochondrial clouds aggregated to one side of the cytoplasm of MOF oocytes (Fig. 5b and c), in contrast with those observed in the follicles having a single oocyte (Fig. 5a). Figures 5d and e show a more developed MOF, where oocytes are separated by follicular epithelial cells or granulosa cells. However, the border structure, such as the basement membrane separating each oocyte is unclear, indicating that oocytes in MOF shared the granulosa cells in the follicles. Furthermore, almost all oocytes of MOFs possessed a clear zona pellucida, but their thickness differed among oocytes (Fig. 5d and e). Unfortunately, we did not find DNOs during observation of ultrathin CR ovary sections by TEM.

Discussion

The ovarian follicle consists of multiple differentiating cell types, while the fundamental core is composed of an oocyte enveloped by granulosa cells. During folliculogenesis, follicular morphology changes as the oocyte grows and the surrounding cells differentiate. The major morphological distinction observed between rodents and other domestic animals is the sheer abundance of primordial follicles located throughout the ovarian cortex, beneath the tunica albuginea. Upon reaching adulthood, the ovaries of common mouse strains contain follicles of varying stages of development in the order of 3,000 to 5,000 [24]. That number declines over time as most follicles die *via* atresia, with a smaller number surviving to ovulation in each estrus cycle. Although PrFs remain arrested and static until the transition from PrF to PF occurs [25], in rodents, the follicular formation occurs fairly synchronously during the first few days after birth, the exact timing depending on species or strains [26]. In this study, we used CRs at 6–8 weeks of age, and their follicular assembly showed that individual oocytes assembled into PrF and each follicle typically consisted of one oocyte.

The most characteristic feature of the CR ovary was the appearance of two or more oocytes in a single follicle, termed as MOFs, which were found in all follicular developmental stages and more frequently in PF and SF. The presence of MOFs in adult ovaries has been reported in mammals [1, 4, 11]. We also investigated the ovaries of C57BL/6N and ICR mice. Here, one MOF was found in a SF and another one in a TF only in ovaries of ICR mice (Supplementary Figs. 1c–d). Moreover, some researchers found MOFs in rodents upon treatment with synthetic estrogenic hormones [27] or the estrogen receptor β agonist 2,3-bis(4-hydroxyphenyl)-propionitrile [28], as well as in ovaries of AQP8 knockout [19] or p27Kip1 mutant mice [29]. Furthermore, the frequency of MOFs differs among species or individuals, with possums showing high incidence of MOFs (e.g. approximately 100 oocytes per follicle), and almost 70% of female dogs having more than one MOF in their ovary [30]. In rabbit ovaries, MOFs were also found in all phases of folliculogenesis, from primary to preovulatory follicles [17]. In humans, binovularity has been defined as the inclusion of two oocytes within a common zona pellucida or their fusion in the zonal region, with no pregnancy being achieved after the transfer of an embryo from a binovular follicle [31]. Although there is no detailed information about the role of MOFs in ovarian physiology, its formation by defective nest breakdown and follicular assembly would most likely contribute to determining the number of MOFs, as reported in rats [18]. Since the appearance of MOFs in CRs decreased in TF compared with PF and SF, almost all of them would disappear until the formation of the antral follicle. However, a few MOFs might be ovulated. It has been suggested that the smallest oocytes in a MOF might be arrested in development and probably degenerate, and all disappear except one, or that all might undergo atresia and never reach the stage of extrusion of the first polar body [32]. Whenever the number of follicles in MOFs was higher than three, they would be present at different developmental stages. Some of these MOFs, where the differences among cells are more pronounced, would possibly undergo degeneration [1]. However, it has also been suggested that MOFs might be ovulated in female dogs [6]. Further studies focusing on the ovulation and fertility features of oocytes derived from MOFs are required to clarify the characteristics of the reproductive function of MOFs.

The frequency of MOFs in the ovaries is species- and individual-dependent (Table 5). In opossum, mice, pigs and goats, MOFs are more common in the ovaries of younger, rather than of older, females [8, 11, 33, 34]. In humans, the frequency of these follicles did not change among different age groups [16] but decreased over time [35].

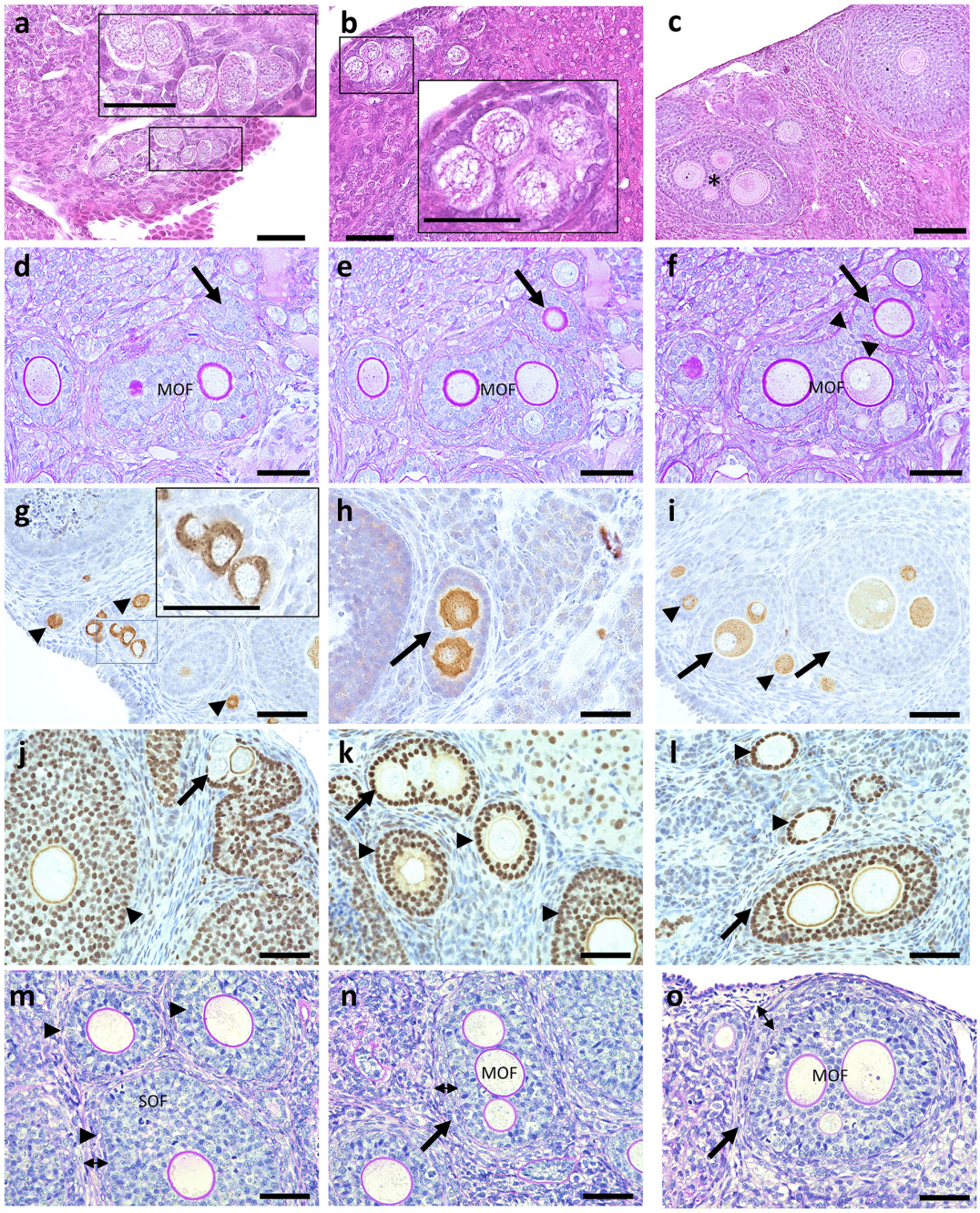

Fig. 3. Unique morphological features of multi-oocyte follicles in the ovary of cotton rats (CRs). (a–c) Histological observation of hematoxylin eosin-stained ovary section in CR at 6–8 weeks of age. More than two oocytes were observed in single follicles classified as primordial (PrF), primary (PF), secondary (SF) (panels a–c, respectively), and each oocyte was separated by follicular epithelial cells or granulosa cells. Squares in panels a–b indicate the same area of the inset. The star in panel c indicates the common granulosa cells (GCs) contained in SF multi-oocyte follicles (MOF). Scale bar = 100 µm. (d–f) Periodic acid Schiff-hematoxylin (PAS-H)-stained semi-serial sections of the ovary in CR at 6–8 weeks of age. Single oocyte follicles (arrows, panels d and e) are connected with near MOF via fine connections of granulosa cells (arrowheads, panel f). Scale bar = 100 µm. (g–i) Immunohistochemistry for the detection of oocyte maker in the ovary of CR at 6–8 weeks of age. DEAD (Asp-Glu-Ala-Asp) box polypeptide 4 (Ddx4)-positive reactions are observed at the cytoplasm of the oocyte in the single oocyte follicles (arrowheads, panels g and i). Ddx4-positive reactions are also observed in the cytoplasm of MOFs classified as PrF (square area), PF and SF (arrows) (panels g–h, respectively). Square area in panel g indicate the same area of the inset. Scale bar = 100 µm. (j-l) Immunohistochemistry for the detection of the follicular epithelial cell marker in the ovary of CR at 6–8 weeks of age. Foxl2 positive reactions are observed at the follicular epithelial cells in the single oocyte follicles (arrowheads, panels j and k) and MOFs (arrows, panel l). Scale bar = 100 µm. (m-o) PAS-H-stained semi-serial sections of the ovary in CR at 6–8 weeks of age. The thickness of the theca cell layer (double arrow heads, panels m, n and o) in single oocyte follicles (arrow heads) and multi-oocyte follicle (arrows). Scale bar = 100 µm.

Table 4. The polarity of single oocyte follicles (SOFs) and multi-oocyte follicles (MOFs) as determined by the measurement of distances (long distance [LD] and short distance [SD]) between the nuclear membrane and the plasma membrane of oocytes in the cotton rat (CR) ovary

Follicle type	PF		SF	
	LD (μm)	SD (μm)	LD (μm)	SD (μm)
SOFs	10.8 ± 0.8 *	7.2 ± 1.0	18.4 ± 1.4 *	12.5 ± 0.8
MOFs	13.9 ± 1.0 #	4.2 ± 0.6	23.6 ± 3.0 #	9.0 ± 1.4

Values are reported as mean ± SE. * and # indicate significant differences between LD and SD, as found by Mann-Whitney *U*-test (* SOF-LD *vs.* SD and # MOF-LD *vs.* SD, $P < 0.01$). n = 50 oocytes (10 randomly selected oocytes/ovary).

The frequency of MOFs in adult CRs was higher in PFs compared to PrFs. Two theories could be put forward to explain the formation of the MOF individually or cooperatively; 1) fusion of developmental follicles or 2) dysregulated oocytogenesis. With regards to theory 1), a recent study suggested the invasive capacity of granulosa cells which could contribute to connecting the follicles and generating the MOFs in the peripubertal rat ovary [18]. However, although the proliferative activity of MOFs was observed by some researchers in mammals [10], Ki-67 staining demonstrated proliferative activity only of GCs but not of oocytes in MOFs of CRs (Supplementary Figs. 2a–c). Interestingly, the MOFs in CRs show two types of morphological characteristics, (i) two or more irregular shaped bulging follicles, projection and migration of granulosa cells into the ovarian stroma, and the shared granulosa cells of these follicles which appear as MOFs, and (ii) adjacent follicles connected by their cytoplasmic bridges appearing as linear forms of MOFs, indicating the invasive capacity of granulosa cells in CRs.

With regards to theory 2), the oogonia can proliferate in fetal mammals and most of them develop to oocytes by the initiation of the first meiotic division. Oogonia are divided synchronously with intercellular bridges between each other due to incomplete cytokinesis [36], with these bridges generally disappearing in oocytes. Therefore, the dysregulated cell division process during oocytogenesis might also contribute to the formation of MOFs. In fact, it has been proposed that MOFs might be derived from the division of a single cell with two or more nuclei formed by amitotic division of the oocyte [31] with failure of oocyte nest breakdown during the early stages of folliculogenesis [2, 10, 11, 37, 38]. Further, the cluster of oocytes surrounded by a common basement membrane is called an oocyte nest and is commonly found in the immature mammalian ovary. The nest breakdown, implying the separation of the nest to each follicle, is observed at the prenatal to neonatal period. Therefore, the dysregulation of this process might also contribute to the production of MOFs in CRs. The other factors might be the encasement of multiple oocytes in PrF during folliculogenesis due to their more rapid developmental rate compared to the differentiation of the surrounding somatic cells [11, 12, 32, 39]. To prove theory 2) in MOF formation, further analysis of the fetal or neonatal CR ovary is required.

The histological analysis of CR ovaries found another typical characteristic of two nuclei being encased in a single follicle, termed as DNOs, among the oocytes of PrF, PF, SF but not in TF. Double nucleated cells can also be observed in other cell types, such as hepatocytes or trophoblasts, and these double nuclei indicate an intensive transcriptional activity [40]. However, DNOs tended to be frequently observed in PrF containing oocytes. The reason for DNO

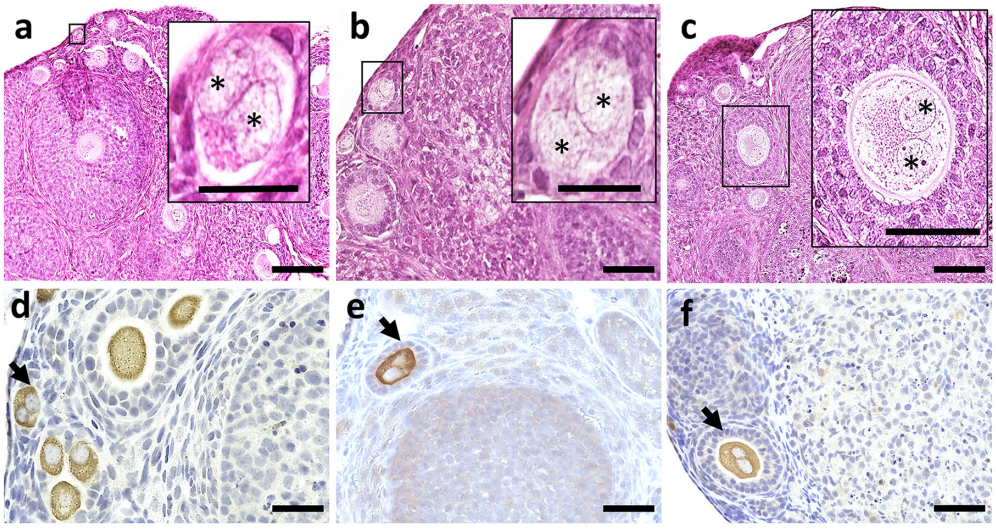

Fig. 4. Double nucleated oocytes in the ovary of cotton rats (CRs). (a–c) Histological observation of hematoxylin eosin-stained ovary section in the CR at 6–8 weeks of age. Two nuclei are observed within a single oocyte in the follicles classified as primordial (PrF), primary (PF), secondary (SF) (panels a–c, respectively). Each nucleus (asterisks) shares the same cytoplasm. (d–f) Immunohistochemistry for the detection of the oocyte maker in the ovary of CR at 6–8 weeks of age. DEAD (Asp-Glu-Ala-Asp) box polypeptide 4 (Ddx4)-positive reactions are observed at the cytoplasm of DNO (arrow) classified as Pr, PF, SF (panels d–f, respectively). Scale bar = 100 μm.

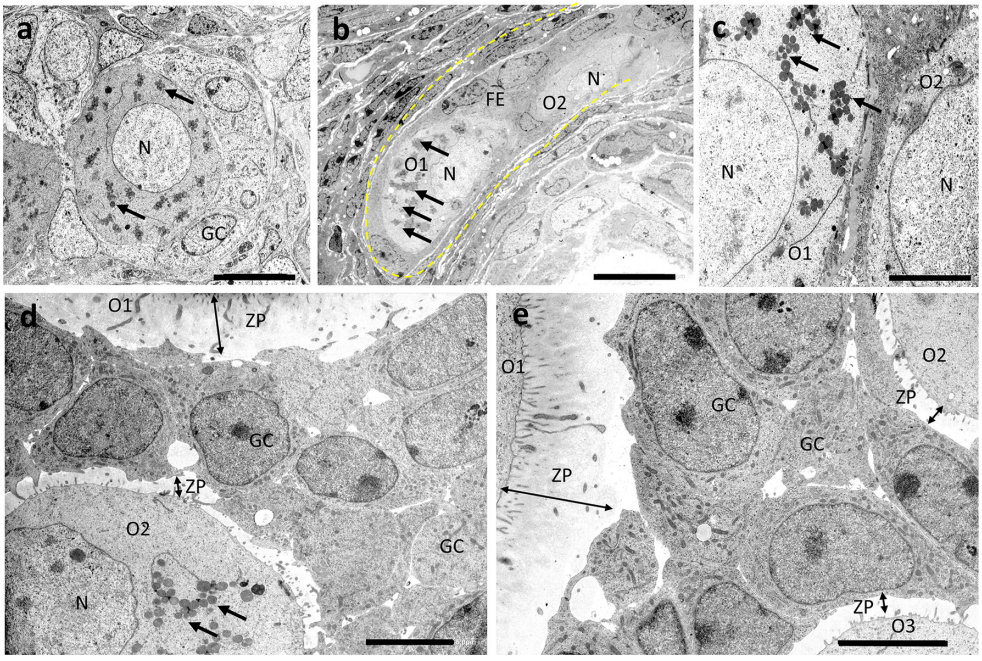

Fig. 5. Ultrastructural features of multi-oocyte follicles in the ovary of cotton rats (CRs). Panels are transmission electron microscopy images of the ovary section of CR at 6–8 weeks of age. Panel a displays a representative primordial (PrF) having a single oocyte with a clear round-shaped nucleus (N) and clouded mitochondria (arrows) distributed throughout the cytoplasm. Panel b shows a multi-oocyte follicles (MOF) classified as PrF. Oocytes (O1 and O2) are separated by follicular epithelial cells (FE). Mitochondrial clouds (arrows) aggregated in the MOF (panels b-c), in contrast with the follicles having a single oocyte (panel a), and they tended to localize to one side of the cytoplasm. Panel d and e show the more developed MOF, and oocytes are separated by granulosa cells (GC). The border structure separating each oocyte is unclear. Oocytes of MOFs in panel d and e possess a clear zona pellucida (ZP), and their thickness differs among oocytes. Scale bar = 5 µm in panels a, b, and c, and 10 µm in panels d and e.

Table 5. Frequency of multi-oocyte follicles (MOFs) in different mammalian species

Animals	Category	Frequency (%) (observed/total follicles)	Reference
Goat	Prepubertal	100.0 (6/6)	Lucci *et al*., 1999
	Non pregnant	50.0 (3/6)	
	Pregnant	17.0 (1/6)	
Dog	Prepubertal	68.4 (13/19)	Payan-Carreira and Pires, 2008
	Mature	36.6 (48/131)	
Pig	Gilts	6.4 (49/819)	Stankiewicz *et al*., 2009
	Sows	1.4 (9/659)	
Cattle	Fetus	40.0 (8/20)	Silva-Santos *et al*., 2011
	Heifer	37.5 (9/24)	
	Cow	45.0 (9/20)	

The table shows previously published data on the frequency of MOFs in 4 mammalian species (goat, dog, pig, cattle).

formation might be: (1) fusion of two individual oogonia during nest breaking; (2) incomplete nuclear division without cytoplasmic cleavage during folliculogenesis; or (3) other unknown factors. Moreover, most DNOs appeared in the early developmental stages of folliculogenesis. There is no report of DNOs in other rodents, but binuclear oocytes are usually found in possum [33]. The prevalence of "polynuclear" follicles was 58% in women under the age of 20 years, whereas similar follicles were found in 13% of women aged 20 to 39 years, and none in the ovaries of women 40 years or older [35]. The previous study suggested that binuclear oocytes in humans might result from the fusion of two individual oogonia or from nuclear division in an oogonium without ensuing cytoplasmic cleavage [41]. CRs might be deficient in these processes, similar to MOF formation.

The ultrastructural analysis of CR ovaries shows that almost all oocytes of MOFs have a clear zona pellucida. The thickness of the zona pellucida in mammals is usually similar among oocytes [1], but that of the MOF differs. These data indicate a partial dysfunction of oocytes in MOFs, even though these can still express the representative oocyte marker Ddx4. This is a characteristic feature of MOFs, although this marker is also expressed in SOFs of CRs. However, the difference in polarity between MOFs and SOFs is clarified ultrastructurally by the presence of mitochondrial clouds in CRs. We hypothesized that such mitochondrial clouds aggregated toward the LD between the nucleus and the plasma membrane. Oocyte polarity and embryonic patterning are well-established features of development in lower species [42]. In particular, the distribution of organelles in oocytes shows dramatic asymmetry resulting in a structural and molecular polarity [43]. However, there is a profound conceptual difference between cell asymmetry and polarity: indeed, the asymmetrical distribution of molecules and/or organelles within a cell does not impose or necessarily indicate the existence of cell polarity [43]. Furthermore, mitochondrial clouds tended to aggregate to one side of the cytoplasm of MOF oocytes**.** These have been termed as Balbiani bodies (Bbs) containing a large RNA-protein granule, and they are universally conserved in the oocytes of insects [44], fish [45], rodents [36], and humans [46]. In all cases, ultrastructural analysis showed that the Bbs were located at the nuclear periphery but at one side of the cytoplasm in MOFs of CRs and were composed of aggregated mitochondria and electron-dense material, likely corresponding to RNA. The Bbs are transient structures, as they only exist in the dormant oocytes, and are dispersed once the oocyte is activated [36]. Although the functional significance of Bbs in CRs is unclear, polarity located Bbs in *Xenopus* oocytes is known to be associated with the germinal granules responsible for the determination of the germ cell fate [47]. In *Xenopus* and mice, Bbs disperse during oocyte growth [36, 48]. Also, in *Xenopus* early oocytes, the microtubules emanate from the centrioles toward the mitochondria of the assembling Bb and are probably involved in the movement and aggregation of mitochondria around the centrioles [48].

This study used the CR animal model and evaluated the unique phenotypes of CR ovaries, which are characterized by the presence of MOFs and DNOs. The data obtained contribute to clarifying how MOFs and DNOs are formed, and also show that the CR is a useful model in studying folliculogenesis and oocytogenesis as well as their abnormalities, in humans and other animals.

Conflict of interest: There are no conflicts of interest to declare.

Acknowledgement

This work was supported by JSPS KAKENHI (Grant No.: JP18K0703708).

References

1. **Payan-Carreira R, Pires MA.** Multioocyte follicles in domestic dogs: a survey of frequency of occurrence. *Theriogenology* 2008; **69**: 977–982. [Medline] [CrossRef]
2. **Oktem O, Urman B.** Understanding follicle growth in vivo. *Hum Reprod* 2010; **25**: 2944–2954. [Medline] [CrossRef]
3. **Tingen C, Kim A, Woodruff TK.** The primordial pool of follicles and nest breakdown in mammalian ovaries. *Mol Hum Reprod* 2009; **15**: 795–803. [Medline] [CrossRef]
4. **Ireland JLH, Scheetz D, Jimenez-Krassel F, Themmen APN, Ward F, Lonergan P, Smith GW, Perez GI, Evans ACO, Ireland JJ.** Antral follicle count reliably predicts number of morphologically healthy oocytes and follicles in ovaries of young adult cattle. *Biol Reprod* 2008; **79**: 1219–1225. [Medline] [CrossRef]
5. **Silva-Santos KC, Santos GMG, Siloto LS, Hertel MF, Andrade ER, Rubin MIB, Sturion L, Melo-Sterza FA, Seneda MM.** Estimate of the population of preantral follicles in the ovaries of Bos taurus indicus and Bos taurus taurus cattle. *Theriogenology* 2011; **76**: 1051–1057. [Medline] [CrossRef]
6. **Reynaud K, de Lesegno CV, Chebrout M, Thoumire S, Chastant-Maillard S.** Follicle population, cumulus mucification, and oocyte chromatin configuration during the periovulatory period in the female dog. *Theriogenology* 2009; **72**: 1120–1131. [Medline] [CrossRef]
7. **Greenwald GS, Moor RM.** Isolation and preliminary characterization of pig primordial follicles. *J Reprod Fertil* 1989; **87**: 561–571. [Medline] [CrossRef]
8. **Stankiewicz T, Blaszczyk B, Udała J.** A study on the occurrence of polyovular follicles in porcine ovaries with particular reference to intrafollicular hormone concentrations, quality of oocytes and their in vitro fertilization. *Anat Histol Embryol* 2009; **38**: 233–239. [Medline] [CrossRef]
9. **Hadek R.** Morphological and histochemical study on the ovary of the sheep. *Am J Vet Res* 1958; **19**: 873–881. [Medline]
10. **Oliveira RL, Silva CB, Silva EO, Gerez JR, Santos MM, Sarapião FD, Sartori L, Bracarense APFRL, Seneda MM.** Proliferative activity of multi-oocyte follicles in sheep ovaries. *Sm Rum Res* 2017; **146**: 58–60. [CrossRef]
11. **Lucci CM, Amorim CA, Rodrigues APR, Figueiredo JR, Báo SN, Silva JRV, Gonçalves PBD.** Study of preantral follicle population in situ and after mechanical isolation from caprine ovaries at different reproductive stages. *Anim Reprod Sci* 1999; **56**: 223–236. [Medline] [CrossRef]
12. **Telfer E, Gosden RG.** A quantitative cytological study of polyovular follicles in mammalian ovaries with particular reference to the domestic bitch (Canis familiaris). *J Reprod Fertil* 1987; **81**: 137–147. [Medline] [CrossRef]
13. **Bristol-Gould S, Woodruff TK.** Folliculogenesis in the domestic cat (Felis catus). *Theriogenology* 2006; **66**: 5–13. [Medline] [CrossRef]
14. **Faith RE, Montgomery CA, Durfee WJ, Aguilar-Cordova E, Wyde PR.** The cotton rat in biomedical research. *Lab Anim Sci* 1997; **47**: 337–345. [Medline]
15. **Ichii O, Nakamura T, Irie T, Kouguchi H, Sotozaki K, Horino T, Sunden Y, Elewa YHA, Kon Y.** Close pathological correlations between chronic kidney disease and reproductive organ-associated abnormalities in female cotton rats. *Exp Biol Med (Maywood)* 2018; **243**: 418–427. [Medline] [CrossRef]
16. **Gougeon A.** Frequent occurrence of multiovular follicles and multinuclear oocytes in the adult human ovary. *Fertil Steril* 1981; **35**: 417–422. [Medline] [CrossRef]
17. **Al-Mufti W, Bomsel-Helmreich O, Christidès JP.** Oocyte size and intrafollicular position in polyovular follicles in rabbits. *J Reprod Fertil* 1988; **82**: 15–25. [Medline] [CrossRef]
18. **Gaytán F, Morales C, Manfredi-Lozano M, Tena-Sempere M.** Generation of multioocyte follicles in the peripubertal rat ovary: link to the invasive capacity of granulosa cells? *Fertil Steril* 2014; **101**: 1467–1476. [Medline] [CrossRef]
19. **Su W, Guan X, Zhang D, Sun M, Yang L, Yi F, Hao F, Feng X, Ma T.** Occurrence of multi-oocyte follicles in aquaporin 8-deficient mice. *Reprod Biol Endocrinol* 2013; **11**: 88. [Medline] [CrossRef]
20. **Yamashita Y, Nakamura T, Otsuka-Kanazawa S, Ichii O, Kon Y.** Morphological characteristics observed during early follicular development in perinatal MRL/MpJ mice. *Jpn J Vet Res* 2015; **63**: 25–36. [Medline]
21. **Francis W, Brambell R.** The development and morphology of the gonads of the mouse. Part III-The growth of the follicles. *Royal Socie* 1997; **103**: 268–272.
22. **Miyabayashi K, Tokunaga K, Otake H, Baba T, Shima Y, Morohashi K.** Heterogeneity of ovarian theca and interstitial gland cells in mice. *PLoS One* 2015; **10**: e0128352. [Medline] [CrossRef]
23. **Tajima K, Orisaka M, Mori T, Kotsuji F.** Ovarian theca cells in follicular function. *Reprod Biomed Online* 2007; **15**: 591–609. [Medline] [CrossRef]
24. **Tilly JL.** Ovarian follicle counts—not as simple as 1, 2, 3. *Reprod Biol Endocrinol* 2003; **1**: 11. [Medline] [CrossRef]
25. **Kezele P, Skinner MK.** Regulation of ovarian primordial follicle assembly and development by estrogen and progesterone: endocrine model of follicle assembly. *Endocrinology* 2003; **144**: 3329–3337. [Medline] [CrossRef]
26. **Fortune JE.** The early stages of follicular development: activation of primordial follicles and growth of preantral follicles. *Anim Reprod Sci* 2003; **78**: 135–163. [Medline] [CrossRef]
27. **Jefferson WN, Couse JF, Padilla-Banks E, Korach KS, Newbold RR.** Neonatal exposure to genistein induces estrogen receptor (ER)alpha expression and multioocyte follicles in the maturing mouse ovary: evidence for ERbeta-mediated and nonestrogenic actions.

Biol Reprod 2002; **67**: 1285–1296. [Medline] [CrossRef]

28. **Sato T, Kim H, Kakuta H, Iguchi T.** Effects of 2,3-*Bis*(4-hydroxyphenyl)-propionitrile on Induction of Polyovular Follicles in the Mouse Ovary. *In Vivo* 2018; **32**: 19–24. [Medline]
29. **Pérez-Sanz J, Arluzea J, Matorras R, González-Santiago N, Bilbao J, Yeh N, Barlas A, Romin Y, Manova-Todorova K, Koff A, de la Hoz C.** Increased number of multi-oocyte follicles (MOFs) in juvenile p27Kip1 mutant mice: potential role of granulosa cells. *Hum Reprod* 2013; **28**: 1023–1030. [Medline] [CrossRef]
30. **Reynaud K, Halter S, Tahir Z, Thoumire S, Chebrout M, Chastant-Maillard S.** Les follicules polyovocytaires. *Gynecol Obstet Fertil* 2010; **38**: 395–397. [Medline] [CrossRef]
31. **Rosenbusch B.** The potential significance of binovular follicles and binucleate giant oocytes for the development of genetic abnormalities. *J Genet* 2012; **91**: 397–404. [Medline] [CrossRef]
32. **Kennedy WP.** The occurrence of polyovular graafian follicles. *J Anat* 1924; **58**: 328–334. [Medline]
33. **Hartman CG.** Polynuclear ova and polyovular follicles in the opossum and other mammals with special reference to the problem of fecundity. *Am J Anat* 1926; **37**: 1–51. [CrossRef]
34. **Davis DE, Hall O.** Polyovuly and anovular follicles in the wild Norway rat. *Anat Rec* 1950; **107**: 187–192. [Medline] [CrossRef]
35. **Dandekar PV, Martin MC, Glass RH.** Polyovular follicles associated with human in vitro fertilization. *Fertil Steril* 1988; **49**: 483–486. [Medline] [CrossRef]
36. **Pepling ME, Wilhelm JE, O'Hara AL, Gephardt GW, Spradling AC.** Mouse oocytes within germ cell cysts and primordial follicles contain a Balbiani body. *Proc Natl Acad Sci USA* 2007; **104**: 187–192. [Medline] [CrossRef]
37. **Safran A, Reubinoff BE, Porat-Katz A, Werner M, Friedler S, Lewin A.** Intracytoplasmic sperm injection allows fertilization and development of a chromosomally balanced embryo from a binovular zona pellucida. *Hum Reprod* 1998; **13**: 2575–2578. [Medline] [CrossRef]
38. **Zeilmaker GH, Alberda AT, van Gent I.** Fertilization and cleavage of oocytes from a binovular human ovarian follicle: a possible cause of dizygotic twinning and chimerism. *Fertil Steril* 1983; **40**: 841–843. [Medline] [CrossRef]
39. **Balciuniene J, Bardwell VJ, Zarkower D.** Mice mutant in the DM domain gene Dmrt4 are viable and fertile but have polyovular follicles. *Mol Cell Biol* 2006; **26**: 8984–8991. [Medline] [CrossRef]
40. **Donne R, Saroul-Aïnama M, Cordier P, Celton-Morizur S, Desdouets C.** Polyploidy in liver development, homeostasis and disease. *Nat Rev Gastroenterol Hepatol* 2020; **17**: 391–405. [Medline] [CrossRef]
41. **Austin CR.** Anomalies of fertilization leading to triploidy. *J Cell Comp Physiol* 1960; **56**(Suppl 1): 1–15. [Medline] [CrossRef]
42. **Edwards RG, Beard HK.** Oocyte polarity and cell determination in early mammalian embryos. *Mol Hum Reprod* 1997; **3**: 863–905. [Medline] [CrossRef]
43. **Wodarz A.** Establishing cell polarity in development. *Nat Cell Biol* 2002; **4**: E39–E44. [Medline] [CrossRef]
44. **Jaglarz MK, Nowak Z, Bilíński SM.** The Balbiani body and generation of early asymmetry in the oocyte of a tiger beetle. *Differentiation* 2003; **71**: 142–151. [Medline] [CrossRef]
45. **Marlow FL, Mullins MC.** Bucky ball functions in Balbiani body assembly and animal-vegetal polarity in the oocyte and follicle cell layer in zebrafish. *Dev Biol* 2008; **321**: 40–50. [Medline] [CrossRef]
46. **Albamonte MI, Albamonte MS, Stella I, Zuccardi L, Vitullo AD.** The infant and pubertal human ovary: Balbiani's body-associated VASA expression, immunohistochemical detection of apoptosis-related BCL2 and BAX proteins, and DNA fragmentation. *Hum Reprod* 2013; **28**: 698–706. [Medline] [CrossRef]
47. **Kloc M, Jaglarz M, Dougherty M, Stewart MD, Nel-Themaat L, Bilinski S.** Mouse early oocytes are transiently polar: three-dimensional and ultrastructural analysis. *Exp Cell Res* 2008; **314**: 3245–3254. [Medline] [CrossRef]
48. **Kloc M, Bilinski S, Dougherty MT, Brey EM, Etkin LD.** Formation, architecture and polarity of female germline cyst in *Xenopus*. *Dev Biol* 2004; **266**: 43–61. [Medline] [CrossRef]